

## keV Neutron Resonance Capture in Barium-137

A. R. de L. Musgrove,<sup>A</sup> B. J. Allen,<sup>A</sup> J. W. Boldeman<sup>A</sup> and R. L. Macklin<sup>B</sup>

<sup>A</sup> AAEC Research Establishment, Private Mail Bag, Sutherland, N.S.W. 2232.

<sup>B</sup> Oak Ridge National Laboratory, Oak Ridge, Tennessee, USA.

### Abstract

The neutron capture cross section of  $^{137}\text{Ba}$  has been measured to high resolution ( $\Delta E/E \approx 0.2\%$ ) below  $E_n = 60$  keV. Average values of resonance parameters, extracted for resonances in the range  $2.7 < E_n < 12$  keV, are as follows: s-wave level spacing  $\langle D \rangle = 380 \pm 70$  eV; s-wave radiative width  $\langle \Gamma_\gamma \rangle_s = 80 \pm 15$  meV; s-wave neutron strength function  $10^4 S_0 = 0.57 \pm 0.2$ ; and p-wave neutron strength function  $10^4 S_1 = 0.45 \pm 0.2$ . The s-wave radiative width and the s-wave neutron strength function appear to be lower for  $^{137}\text{Ba}$  than for the other barium isotopes.

### Introduction

This paper reports on measurements of the neutron capture cross section of  $^{137}\text{Ba}$  made at the Oak Ridge Electron Linear Accelerator (ORELA) using the 40 m flight path. The energy resolution achieved was of the order of  $0.2\%$ , and most of the s-wave and p-wave resonances between 2.7 and 12 keV were detected. The present report concludes our study of neutron radiative capture in the isotopes of barium (Musgrove *et al.* 1974, 1975, 1976), and provides further information on the variation of average resonance parameters near the closed neutron shell  $N = 82$ . There was an early suggestion that the radiative widths showed an even-odd effect (Chevillon-Pitollat 1967), and recent transmission measurements by Van der Vyver and Pattenden (1971) indicated a considerable variation in the s-wave neutron strength functions of the barium isotopes.

We previously reported on the neutron capture mechanism in  $^{138}\text{Ba}$  (Musgrove *et al.* 1975) which appears to be dominated by nonstatistical processes and leads to a considerably enhanced s-wave radiative width for this isotope. There was also a suggestion (Musgrove *et al.* 1976) that radiative capture in  $^{136}\text{Ba}$  also displayed certain nonstatistical aspects. In particular, the p-wave radiative width appeared to be considerably larger than the s-wave radiative width. Since  $^{137}\text{Ba}$  is an odd- $A$  target nucleus, nonstatistical effects are expected to be minimized relative to the even- $A$  neighbouring isotopes. However, the proximity to the closed shell may affect the magnitude of the radiative width and neutron strength function relative to the other odd- $A$  nucleus  $^{135}\text{Ba}$ , which was the subject of an earlier investigation (Musgrove *et al.* 1974). The present data supersede the preliminary results of Allen *et al.* (1974).

### Experimental Details

The present experiment was performed at the 40 m station of ORELA, the capture  $\gamma$  rays being detected by a symmetrically situated pair of nonhydrogenous liquid

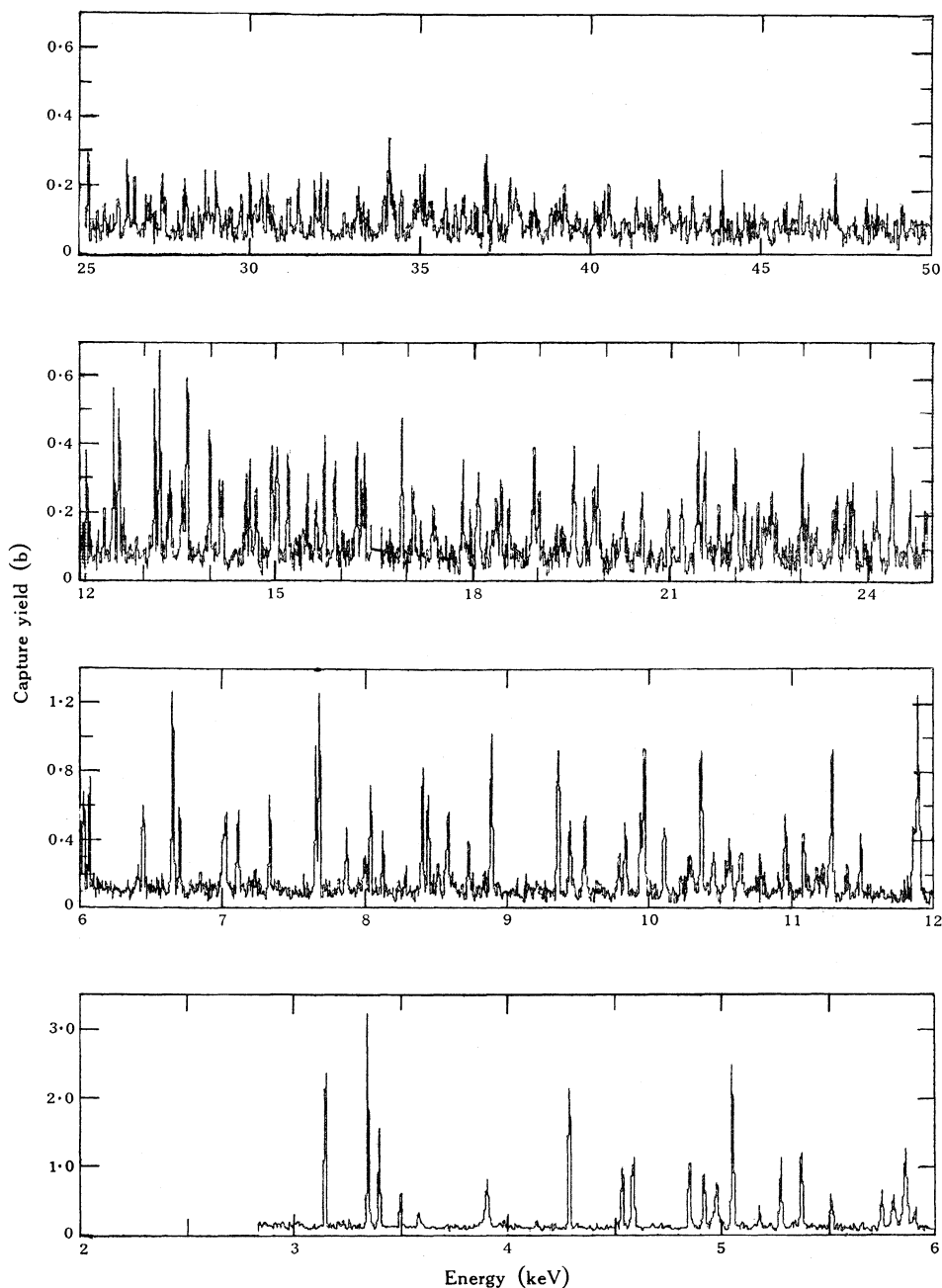


Fig. 1. Uncorrected capture yield data for  $^{137}\text{Ba}$  for bombarding energies between 3 and 50 keV.

scintillators with small sensitivity to scattered neutrons. A calculated pulse height weighting scheme ensured that the detector response was proportional, on average, to the total energy of the capture event. The detector efficiency was normalized using the saturated resonance technique for the 4.9 eV resonance in  $^{197}\text{Au}$ . Further details of the experimental arrangement and detectors can be found in previous articles (Macklin 1971; Macklin and Allen 1971; Allen *et al.* 1973).

Table 1.  $^{137}\text{Ba}$  resonance parameters for 2.7–12 keVParenthesized  $l$ -values correspond to a confidence level of <85% for the particular separation

Energy (keV)	$A_\gamma$ (b eV)	$g\Gamma_n\Gamma_\gamma/\Gamma$ (meV)	$\Gamma_n$ (eV)	$l$	$g$	$\Gamma_\gamma$ (meV)	$\Gamma_n^0$ (meV)	$g\Gamma_n^1$ (meV)
3.146±0.002	33.0	25±4	~0.5	(0)	(0.375)	~77	~9	
3.346±0.002	40.3	32±5	~0.5	(0)	(0.625)	~58	~9	
3.398±0.002	15.2	12±2		(1)				52
3.498±0.002	5.9	5±1		1				16
3.584±0.002	2.1	2±1		1				5
3.905±0.002	24.8	23±4	5±1	0	(0.375)	63±10	80	
4.288±0.002	34.8	36±5	2 $^{+1}_{-0.5}$	(0)	(0.625)	61±10	30	
4.537±0.002	11.1	12±2		1				32
4.581±0.002	9.1	10±2		1				25
4.590±0.002	10.4	12±2		1				30
4.851±0.002	14.3	17±3		(1)				46
4.918±0.002	11.2	13±2		(1)				32
4.977±0.002	24.3	29±5	5±1	0	(0.375)	79±15	71	
5.053±0.002	32.7	40±5	(0.5)	0	(0.625)	~73	(7)	
5.177±0.002	3.0	4±2		1				6
5.278±0.002	12.9	16±3		(1)				40
5.374±0.002	14.8	19±3		(0)			1	
5.514±0.002	7.5	10±2		1				19
5.753±0.002	7.9	11±2		1				20
5.806±0.002	16.2	23±4	8±2	0	(0.375)	61±10	105	
5.862±0.002	47.8	68±8	6±2	0	(0.625)	110±20	78	
6.025±0.004	10.2	15±3		(1)				28
6.066±0.004	10.0	15±3		(1)				27
6.444±0.004	8.9	14±2		(1)				23
6.652±0.004	18.7	30±4		(0)			1	
6.702±0.004	8.2	13±3		1				20
7.017±0.004	32.7	55±6	14±3	0	(0.625)	89±15	167	
7.112±0.004	8.6	15±3		(1)				22
7.334±0.004	10.5	19±4		(1)				29
7.657±0.004	12.6	23±4		(0)				
7.680±0.004	18.4	34±5		(0)				
7.827±0.004	7.4	14±3		1				17
8.000±0.004	5.4	10±2		1				11
8.040±0.004	9.7	19±4						
8.125±0.004	4.8	9±2		1				10
8.405±0.004	12.0	24±4						
8.447±0.004	11.1	23±4						
8.522±0.004	3.5	7±2		1				6
8.583±0.004	14.1	29±5		(0)				
8.729±0.004	5.8	12±3		1				12
8.889±0.004	21.6	46±7	(1)	0	(0.625)	~80		
9.358±0.004	20.3	46±6	(1)	0	(0.625)	~80		
9.441±0.004	8.2	19±4						
9.546±0.004	9.3	21±4						
9.786±0.004	5.0	12±2						
9.831±0.004	7.6	18±3						
9.938±0.004	11.3	27±5						
9.963±0.004	21.3	51±8	(1)	0	(0.625)	~89		

Table 1 (Continued)

Energy (keV)	$A_\gamma$ (b eV)	$g\Gamma_n\Gamma_\gamma/\Gamma$ (meV)	$\Gamma_n$ (eV)	$l$	$g$	$\Gamma_\gamma$ (meV)	$\Gamma_n^0$ (meV)	$g\Gamma_n^1$ (meV)
10·11±0·005	14·2	34±5	4±2	0	(0·375)	94±20	~40	
10·29±0·005	17·1	42±7	20±5	0	(0·625)	68±15	197	
10·37±0·005	22·3	56±8		0				
10·45±0·005	7·3	18±3						
10·54±0·005	4·2	11±2						
10·56±0·005	5·2	13±3						
10·64±0·005	6·8	18±4						
10·78±0·005	4·9	13±4						
10·96±0·005	12·3	33±6		(0)				
11·09±0·005	8·2	22±4						
11·22±0·005	5·8	16±4						
11·28±0·005	21·1	57±8		(0)				
11·49±0·005	6·2	17±3						
11·87±0·005	13·4	38±6		(0)				
11·90±0·005	38·1	109±20	~5	0	(0·625)	~181	~46	

The integrated neutron yield at the source was measured using a communal time-gated fission detector. Some time after completion of the present experiment, a thin (0·5 mm)  $^6\text{Li}$  glass neutron flux monitor was inserted in the beam at 39·5 m and the  $^6\text{Li}(n, \alpha)$  yield was measured. The  $^{137}\text{Ba}$  data were then normalized to the standard  $^6\text{Li}(n, \alpha)$  cross section (Uttley *et al.* 1971; Fort and Marquette 1972; Poenitz 1974) using the ratio of the two fission monitor counts. Over short time scales, normalizations relying on the fission monitor ratio have proved accurate to within ~10% (Allen *et al.* 1973*b*; Musgrove *et al.* 1975, 1976). In the present experiment, however, the elapsed time between measurement of the  $^{137}\text{Ba}$  capture yield and the  $^6\text{Li}(n, \alpha)$  yield may raise some doubts about the reliability of this normalization.

The long term stability of the fission monitor was checked by reference to a run on  $^{48}\text{Ti}$ , which was performed just before the  $^{137}\text{Ba}$  measurement with identical machine-operating conditions, and which was recently remeasured relative to the  $^6\text{Li}(n, \alpha)$  cross section. The two titanium runs agreed to within 12%, so it is reasonable to expect that the absolute normalization error for the  $^{137}\text{Ba}$  will be  $\lesssim 15\%$ . By comparison, the statistical errors in the measured capture areas are typically ~5% and can be ignored. The machine operated with an 8 ns pulse width of repetition rate  $500\text{ s}^{-1}$ , and the target was an isotopically enriched sample of  $\text{BaCO}_3$  (89·6%  $^{137}\text{Ba}$ ; 0·0116 at.  $\text{b}^{-1}$ ).

## Data Analysis

The resonance analysis was performed using a locally modified version of the ORNL-RPI Monte Carlo code (Sullivan *et al.* 1969) to fit resonance capture areas and correct for self-shielding and multiple-scattering effects in the target. Self-shielding corrections were quite large for this target, reaching 50% for the larger resonances, while the multiple-scattering corrections were always negligible by comparison. The quantity obtained from the area fit is the thin sample capture area  $A_\gamma = 2\pi^2\lambda^2 g\Gamma_n\Gamma_\gamma/\Gamma$ , where  $g$  is the spin weighting factor, and  $\Gamma_n$ ,  $\Gamma_\gamma$  and  $\Gamma$  are respectively the neutron, radiative and total resonance widths. The resonance

parameter part of  $A_\gamma$ , denoted by  $\kappa = g\Gamma_n\Gamma_\gamma/\Gamma$ , provides estimates for  $g\Gamma_\gamma$  when  $\Gamma_n \gg \Gamma_\gamma$  and for  $g\Gamma_n$  when  $\Gamma_\gamma \gg \Gamma_n$ . For some resonances, the neutron widths were extracted by shape analysis, this being possible when  $\Gamma_n > 0.3\Gamma_R$ , where  $\Gamma_R$  is the FWHM of the resolution function. Further crude estimates for  $\Gamma_n$  were made for some unresolved resonances which appeared likely to have neutron widths in the range  $0.3\Gamma_R > \Gamma_n > \Gamma_\gamma$ .

Fig. 1 displays the capture yield data obtained between 3 and 50 keV, and Table 1 provides details of the resonances analysed below 12 keV. The  $l$  values recommended in Table 1 were determined from a Bayes theorem analysis as described by Musgrove *et al.* (1974), while the  $g$  values have been assigned tentatively from the observed value for  $g\Gamma_\gamma$  on assuming  $\langle\Gamma_\gamma\rangle$  to be independent of  $J$ . For  $^{137}\text{Ba}$  the target spin is  $3/2^+$ , so that s-wave neutrons capture into states with  $J = 2$  ( $g = 0.625$ ) or  $J = 1$  ( $g = 0.375$ ). The disparity in  $g$  values allows  $J$  assignments to be made for the s-wave resonances with  $\Gamma_n \gg \Gamma_\gamma$ .

**Table 2. Average resonance parameters for isotopes of barium**  
Data are from Musgrove *et al.* (1974, 1975, 1976) and the present work

Parameter	$^{134}\text{Ba}$	$^{135}\text{Ba}$	$^{136}\text{Ba}$	$^{137}\text{Ba}$	$^{138}\text{Ba}$
$\langle D \rangle$ (eV)	$127 \pm 10$	$39.3 \pm 4$	$\sim 1000$	$380 \pm 70$	$7500 \pm 1500$
$\langle \Gamma_\gamma \rangle_s$ (meV)	$120 \pm 20$	$150 \pm 20$	$125 \pm 30$	$80 \pm 15$	$310 \pm 25$
$10^4 S_0$	$0.85 \pm 0.03$	$1.0 \pm 0.2$	$\sim 1.0$	$0.57 \pm 0.2$	$0.9 \pm 0.4$
$10^4 S_1$	$\sim 0.8$	$0.8 \pm 0.2$	—	$0.45 \pm 0.2$	$\sim 0.5$
$\langle \sigma.v \rangle / v_T$ (mb)	$225 \pm 35$	$300 \pm 60$	$61 \pm 10$	$53 \pm 10$	$5 \pm 2$

#### Average s-Wave Resonance Parameters

Fig. 2 gives a staircase plot of the s-wave level sequence below 8 keV, where  $l$  assignments were reasonably unambiguous. From the best straight line fit, the average s-wave level spacing is  $\langle D \rangle = 380 \pm 70$  eV. The quoted error derives from an estimated uncertainty of  $\pm 2$  in the level count.

Previous measurements of the total cross section for  $^{137}\text{Ba}$  below  $\sim 2$  keV have identified eight levels having an apparent spacing of about 230 eV (Alves *et al.* 1969; Van der Vyver and Pattenden 1971). It is possible that some resonances are mis-assigned in our data, and it is probable that some of the resonances found in the total cross section are p wave. For example, a Bayes theorem analysis of the reported resonances near 1 keV indicates that both are probably p-wave resonances. We attempted to add further resonances to the s-wave sequence and found it difficult to retain agreement with the Porter–Thomas and the Wigner distributions for the reduced neutron widths and the level spacings respectively. Fig. 3 gives a diagram of the cumulative s-wave reduced neutron widths compared with the Porter–Thomas distribution; the agreement is good, indicating that few levels have been missed below 8 keV.

The s-wave neutron strength function calculated for the  $^{137}\text{Ba}$  resonances listed in Table 1 is

$$S_0 = \sum g\Gamma_n^0/\Delta E = (0.57 \pm 0.2) \times 10^{-4},$$

which supports the low value obtained from the previously observed levels below 2 keV ( $10^4 S_0 = 0.33 \pm 0.17$ ). This is the smallest neutron strength function found

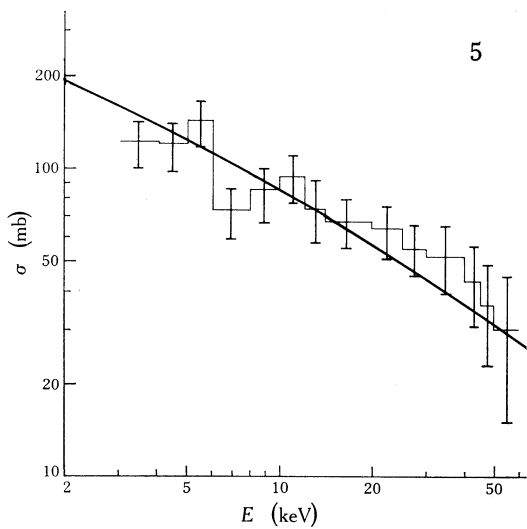
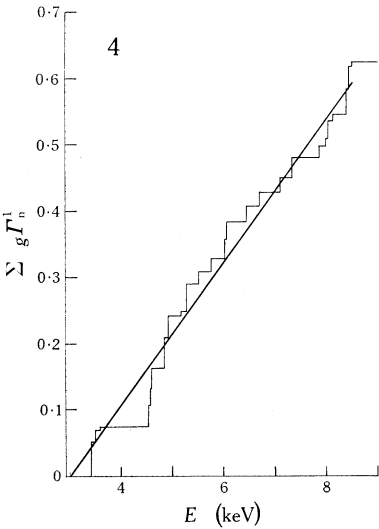
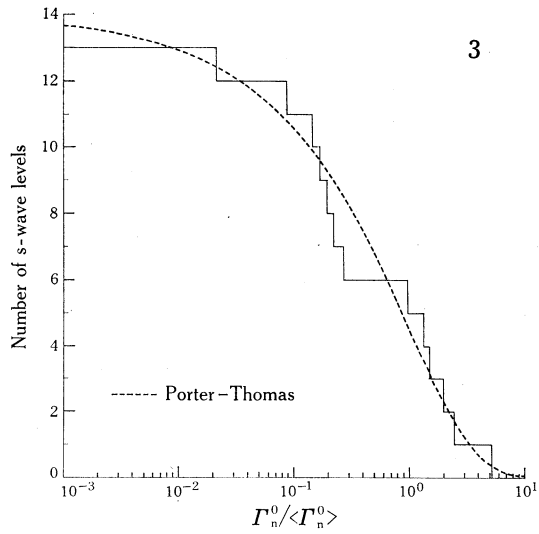
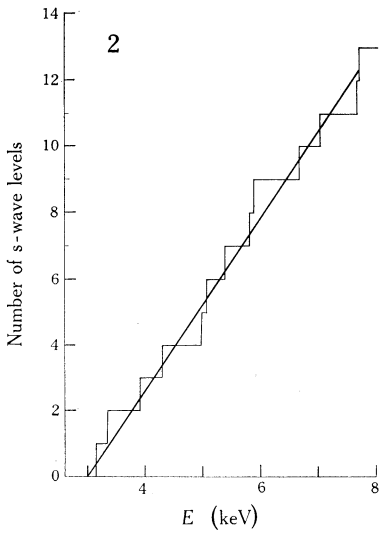


**Fig. 2.** Staircase plot showing the cumulative number of s-wave levels for energies below a given value  $E$  up to 8 keV. The straight line of best fit indicates an average level spacing of  $\langle D \rangle = 380 \pm 70$  eV.

**Fig. 3.** Descending staircase plot showing the cumulative number of s-wave levels for s-wave reduced neutron widths above a given value  $\Gamma_n^0 / \langle \Gamma_n^0 \rangle$ . The Porter-Thomas distribution predicts 14 s-wave levels below 8 keV, as against the observed 13 levels.

**Fig. 4.** Staircase plot showing the cumulative p-wave reduced neutron widths  $\sum g\Gamma_n^1$  for energies below a given value  $E$  up to 9 keV. The straight line of best fit indicates an average p-wave neutron strength function of  $S_1 = (0.36 \pm 0.15) \times 10^{-4}$ .

**Fig. 5.** Comparison of the experimental capture cross section  $\sigma$  for  $^{137}\text{Ba}$  below 60 keV with a statistical model calculation (curve) based on the following average parameters:  $\langle D \rangle = 380$  eV,  $\langle \Gamma_\gamma(s) \rangle = 80$  meV,  $\langle \Gamma_\gamma(p) \rangle = 100$  meV,  $S_0 = 0.57 \times 10^{-4}$ ,  $S_1 = 0.55 \times 10^{-4}$ .

among the barium isotopes as can be seen from Table 2, which compares average resonance parameters obtained here for  $^{137}\text{Ba}$  with those for other barium isotopes. Maxwellian averaged 30 keV capture cross sections  $\langle\sigma \cdot v\rangle/v_T$  are included as these are of particular astrophysical importance.

The average s-wave radiative width is found to be  $\langle\Gamma_\gamma\rangle_s = 80 \pm 15$  meV with  $\pm 15\%$  systematic error. Again, this is lower than the average s-wave radiative widths observed for the other barium isotopes (see Table 2).

#### *p-Wave Neutron Strength Function*

For the small p-wave levels given in Table 1, a value for  $g\Gamma_n$  has been extracted assuming an average p-wave radiative width of 100 meV. Fig. 4, which is a cumulative plot of these values below 9 keV, indicates a value for the neutron strength function of

$$S_1 = \sum g\Gamma_n^1/3\Delta E = (0.36 \pm 0.15) \times 10^{-4}.$$

However, several p-wave levels have evidently been missed. If the level density is proportional to the usual  $2J+1$  factor, p-wave resonances should be twice as numerous as s-wave resonances. Therefore, about six p-wave resonances are probably missed below 8 keV, and this will increase the estimated p-wave neutron strength function somewhat. Also, if the p-wave radiative width were smaller than the assumed value, the deduced strength function would be larger.

#### *Average Cross Section over 3–60 keV*

The average capture cross section below 60 keV is shown collapsed into broad energy intervals in Fig. 5, in which the error bars reflect the normalization error. Above 12 keV, the cross section was determined by subtracting a linear background, integrating the capture yield and making an average correction for self-shielding. A further error is introduced into the cross sections owing to error in estimating the background above  $\sim 30$  keV.

The curve in Fig. 5 shows the results of a statistical model calculation of the capture cross section for a p-wave neutron strength function  $S_1 = 0.55 \times 10^{-4}$ , which is somewhat greater than the value found from the resonances. The actual p-wave strength function may be intermediate between these extremes and we recommend

$$10^4 S_1 = (0.45 \pm 0.2) \pm 15\%.$$

The normalization error enters here since p-wave neutron widths depend almost linearly on the capture areas. The p-wave strength function is lower than the value of  $10^4 S_1 = 0.8$  obtained for  $^{135}\text{Ba}$  (see Table 2).

It is evident that there is a significant decrease in both the radiative width and the neutron strength function for  $^{137}\text{Ba}$  relative to the other isotopes, e.g. the s-wave radiative width for the closed shell nucleus  $^{138}\text{Ba}$  is more than three times that found for  $^{137}\text{Ba}$ . These smaller values for  $^{137}\text{Ba}$  relative to the other isotopes of barium, and particularly  $^{135}\text{Ba}$ , could be caused by a sudden reduction in the density of available doorway states at the closed shell  $N = 82$ , as discussed by Block and Feshbach (1963). Fluctuations in the coupling between the entrance channel state and the doorway state configurations cause local divergences away from the predicted

optical model strength functions. Investigations in the 3s region (Müller and Röhr 1971) and the 4s region (Kirouac 1975) have disclosed significant odd-even fluctuations in s-wave neutron strength functions.

### Acknowledgment

This work is sponsored in part by ERDA under contract to Union Carbide Corporation.

### References

- Allen, B. J., Chan, D. M. H., Musgrove, A. R., and Macklin, R. L. (1974). Proc. Sov. Natl Conf. on Neutron Physics, Kiev, Vol. 2, p. 275.
- Allen, B. J., Macklin, R. L., Winters, R. R., and Fu, C. Y. (1973*b*). *Phys. Rev. C* **8**, 1504.
- Alves, R. N., de Barros, S., Chevillon, P. L., Julien, J., Morgenstern, J., and Samour, C. (1969). *Nucl. Phys. A* **134**, 118.
- Block, B., and Feshbach, H. (1963). *Ann. Phys. (New York)* **23**, 47.
- Chevillon-Pitollat, P. L. (1967). C.E.N (Saclay) Rep. No. CEA-R-3128.
- Fort, E., and Marquette, J. P. (1972). Proc. 2nd IAEA Panel on Neutron Standard Reference Data, Vienna, p. 113 (IAEA: Vienna).
- Kirouac, G. J. (1975). Proc. Conf. on Nuclear Cross Sections and Technology, Washington (Eds R. A. Schrack and C. D. Bowman), Vol. 1, p. 360 (U.S. Govt: Washington, D.C.).
- Macklin, R. L. (1971). *Nucl. Instrum. Methods* **91**, 79.
- Macklin, R. L., and Allen, B. J. (1971). *Nucl. Instrum. Methods* **91**, 565.
- Müller, K-N., and Röhr, G. (1971). *Nucl. Phys. A* **164**, 97.
- Musgrove, A. R., Allen, B. J., Boldeman, J. W., and Macklin, R. L. (1975). *Nucl. Phys. A* **252**, 301.
- Musgrove, A. R., Allen, B. J., Boldeman, J. W., and Macklin, R. L. (1976). *Nucl. Phys. A* **256**, 173.
- Musgrove, A. R., Allen, B. J., and Macklin, R. L. (1974). AAEC Rep. No. AAEC/E327.
- Poenitz, W. P. (1974). *Z. Phys. B* **26**, 359.
- Sullivan, J. G., Warner, G. C., Block, R. C., and Hockenbury, R. W. (1969). Rensselaer Polytech. Inst. Rep. No. RPI-328-166.
- Uttley, C. A., Sowerby, M. G., Patrick, B. H., and Rae, E. R. (1971). Conf. on Neutron Cross Sections and Technology, CONF-710301, Knoxville (Ed. R. L. Macklin), Vol. 1, p. 551 (Univ. Tennessee Press).
- Van der Vyver, R. E., and Pattenden, N. J. (1971). *Nucl. Phys. A* **177**, 393.